Supporting Information

Tampering with Molecular Cohesion in Crystals of Hexaphenylbenzenes

Eric Gagnon,[†] Shira D. Halperin,[‡] Valérie Métivaud,[†]

Kenneth E. Maly,[‡] and James D. Wuest[†*]

[†]*Département de Chimie, Université de Montréal, Montréal, Québec H3C 3J7 Canada*

[‡]*Department of Chemistry, Wilfrid Laurier University, Waterloo, Ontario N2L 3C5 Canada*

Content	Page

*Author to whom correspondence may be addressed: *james.d.wuest@umontreal.ca*

Figure S1. ORTEP view of the structure of crystals of 1-(2-methylphenyl)-2,3,4,5,6-pentaphenylbenzene (**3b**) grown from chlorobenzene. The ellipsoids of non-hydrogen atoms are drawn at the 30% probability level, and hydrogen atoms are represented by a sphere of arbitrary size.
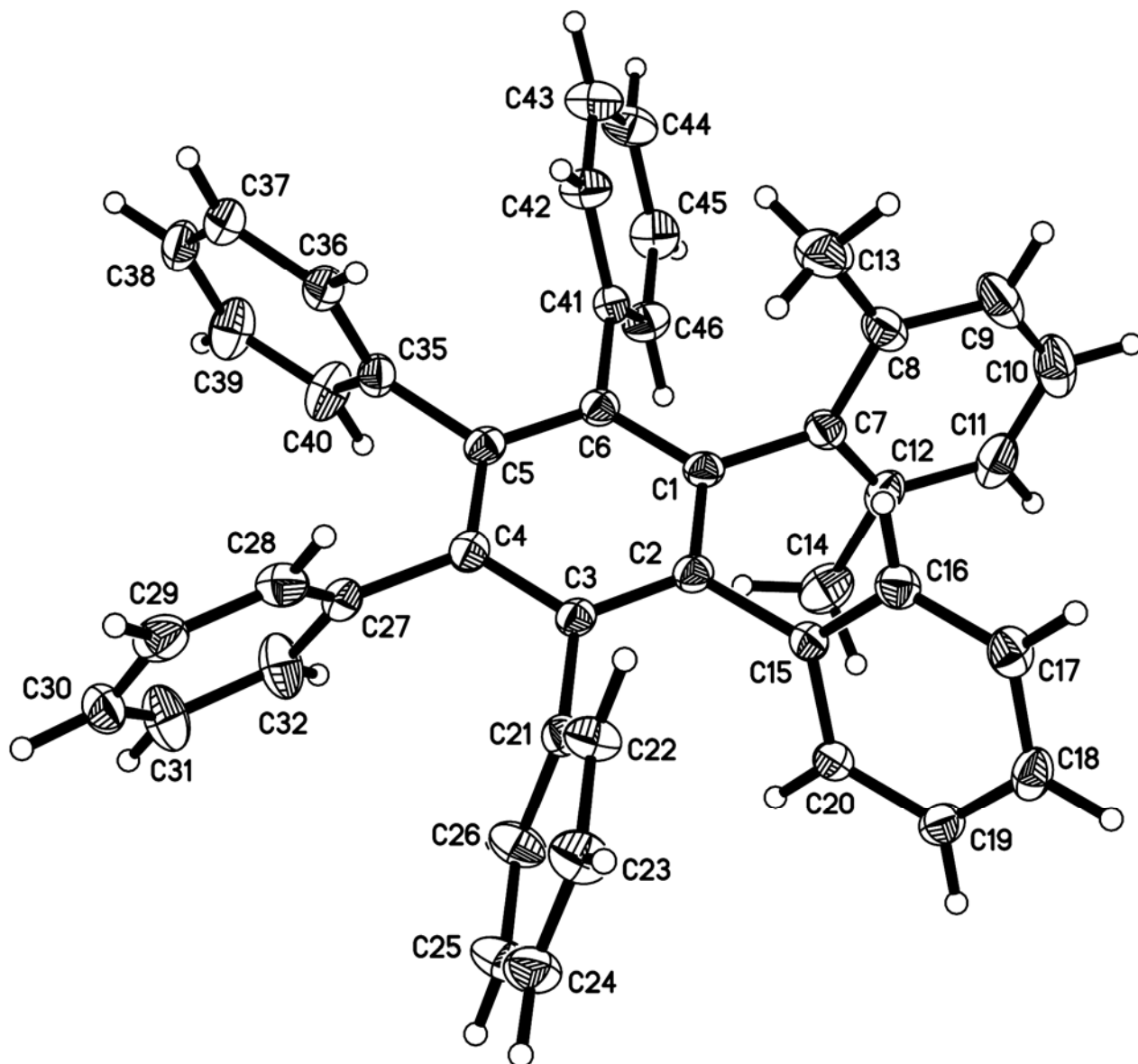
Figure S2. ORTEP view of the structure of crystals of 1-(2,6-dimethylphenyl)-2,3,4,5,6-pentaphenylbenzene (**3c**) grown from toluene. The ellipsoids of non-hydrogen atoms are drawn at the 30% probability level, and hydrogen atoms are represented by a sphere of arbitrary size.

Figure S3. ORTEP view of the structure of crystals of 1-(2,6-diethylphenyl)-2,3,4,5,6-pentaphenylbenzene (**3d**) grown from toluene/hexanes. The ellipsoids of non-hydrogen atoms are drawn at the 30% probability level, and hydrogen atoms are represented by a sphere of arbitrary size.
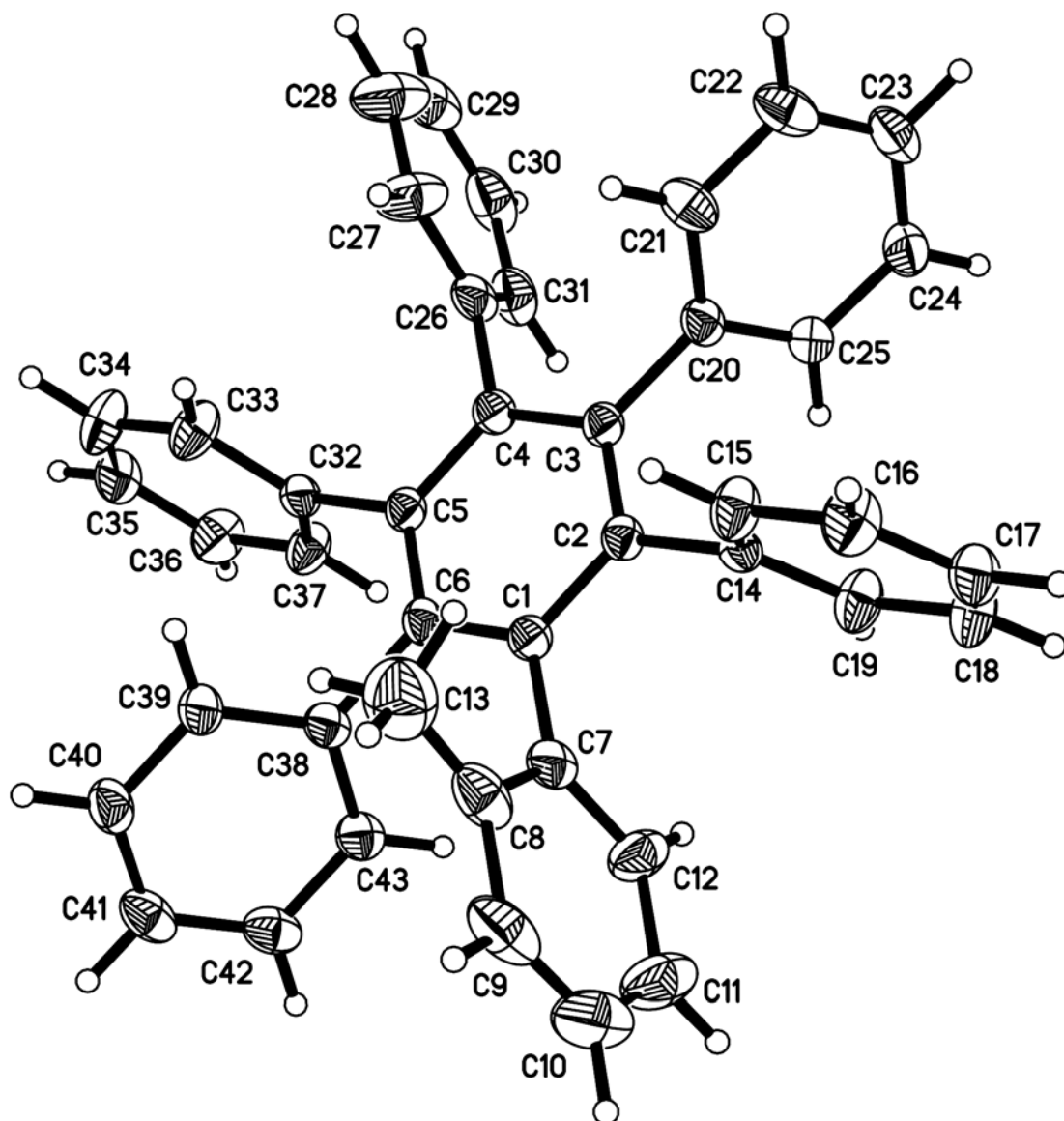
Figure S4. ORTEP view of the structure of crystals of 1-(2,6-diisopropylphenyl)-2,3,4,5,6-pentaphenylbenzene (**3e**) grown from toluene/hexanes. The ellipsoids of non-hydrogen atoms are drawn at the 30% probability level, and hydrogen atoms are represented by a sphere of arbitrary size.
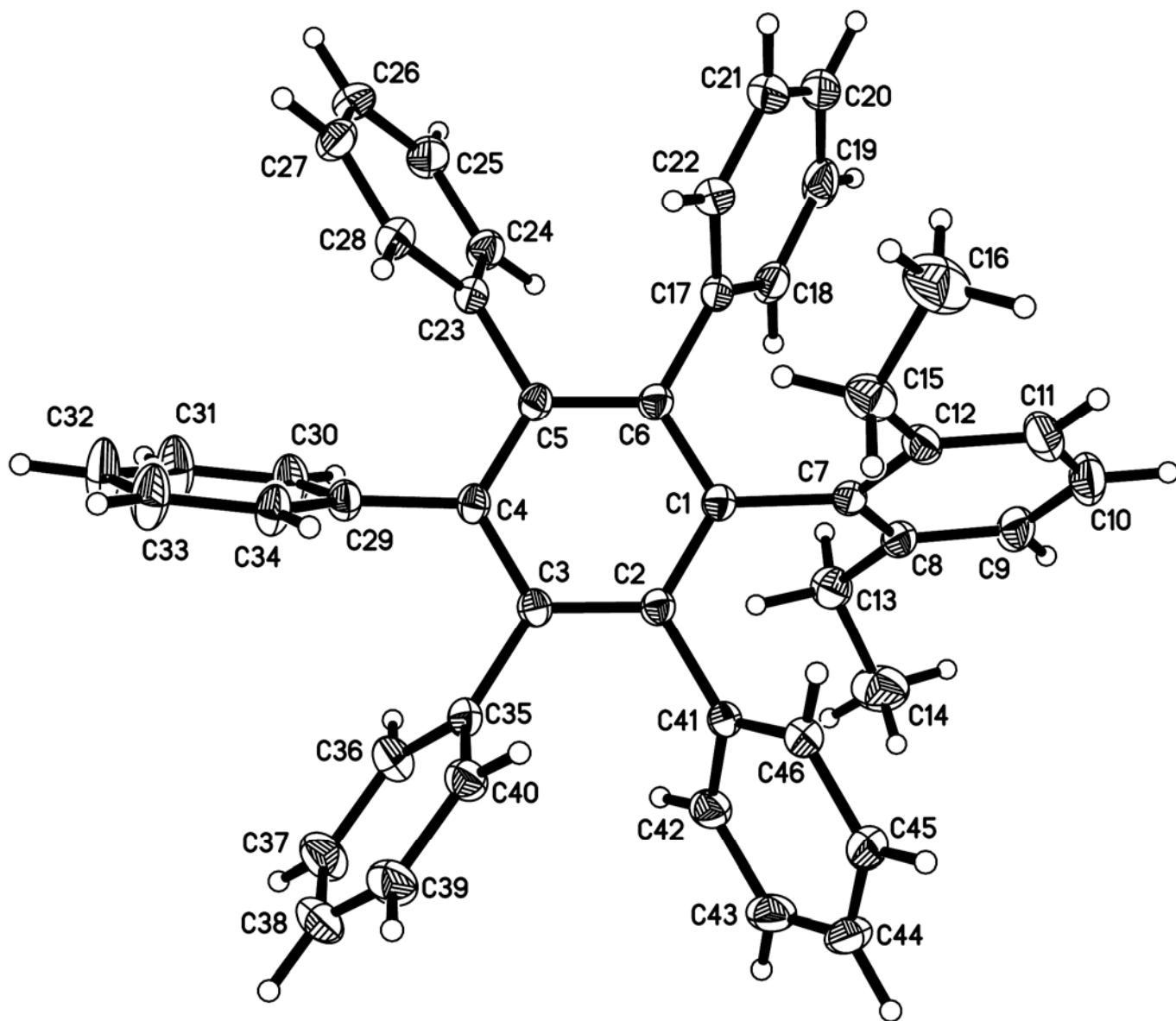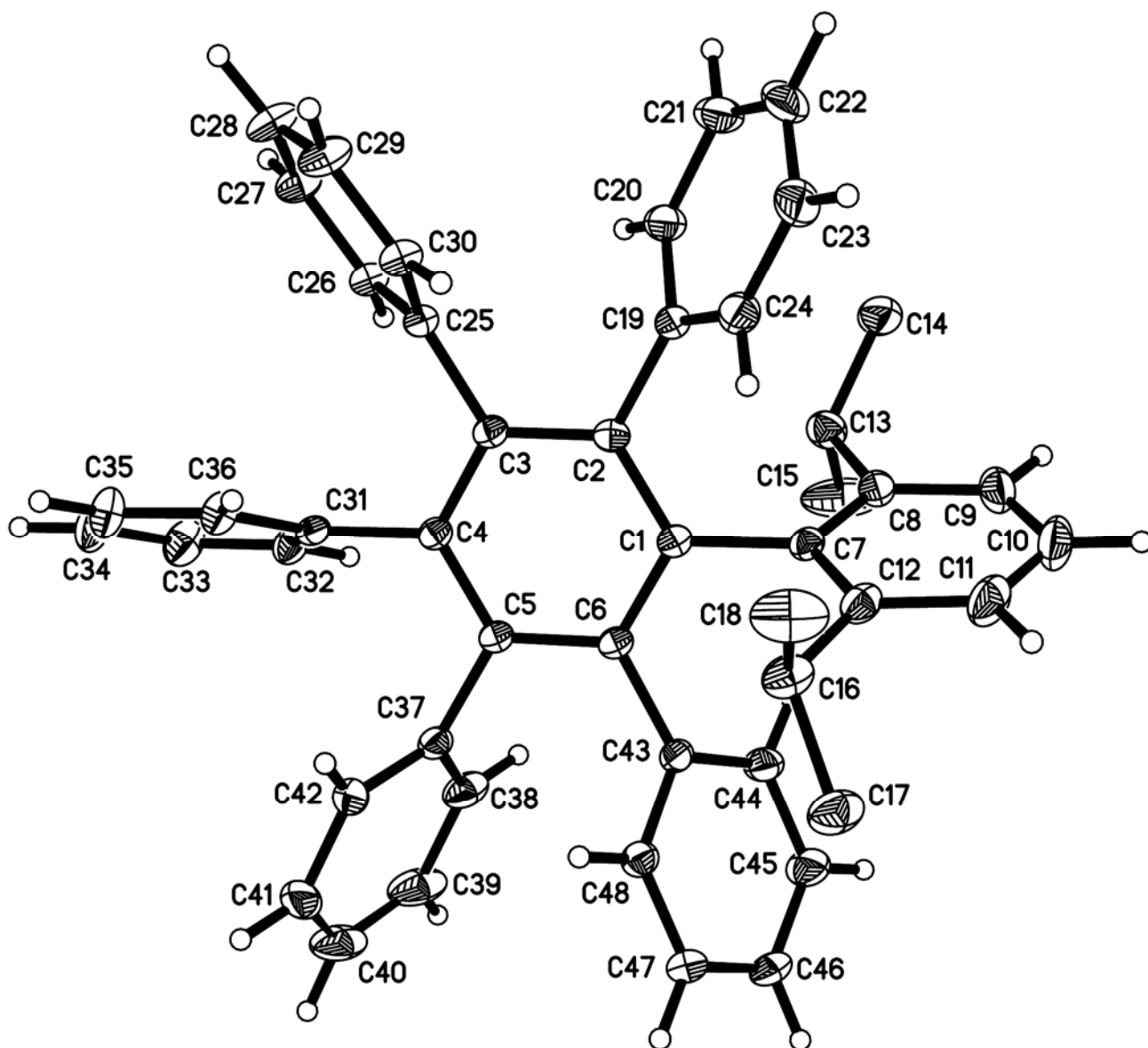
Homogeneity of Bulk Crystalline Samples

In all structural studies, experimental powder X-ray diffraction patterns were recorded for each bulk crystalline sample and then compared with those calculated from single-crystal X-ray diffraction data. In all cases, these comparisons confirmed that the single-crystal specimens selected for structural analysis were representative of the bulk crystalline samples from which they were chosen.

Experimental powder X-ray diffraction patterns were recorded at 25 ºC in reflection mode on a Bruker D8 Advance powder X-ray diffractometer equipped with a VÅNTEC-1 linear position-sensitive detector, using Ge-monochromatized Cu Kα_1 radiation generated at 40 kV and 40 mA. Calibration of the instrument was done with a NIST 1976 corundum sample. For each experiment, the bulk crystalline sample was ground, the resulting powder was placed in a sample holder (PMMA holder ring), and the surface of the powder was flattened with a glass plate. Data were collected in Bragg-Brentano geometry in the range 2° < 2θ < 50° with a step size of 0.016º and a counting time of 2s/step.

Structural data from single-crystal analyses were used to calculate theoretical powder X-ray diffraction patterns with the aid of Mercury software. Peak fitting and the refinement of lattice parameters were carried out using TOPAS software (Bruker), and Pawley fitting was applied to the powder X-ray diffraction patterns. All experimental and calculated diffraction patterns were plotted in the most pertinent range (5° < 2θ < 35°). The x-scale of the experimental pattern was shifted to minimize the slight angular shift due to the effect of temperature.

PXRD Data for Compound **3b**
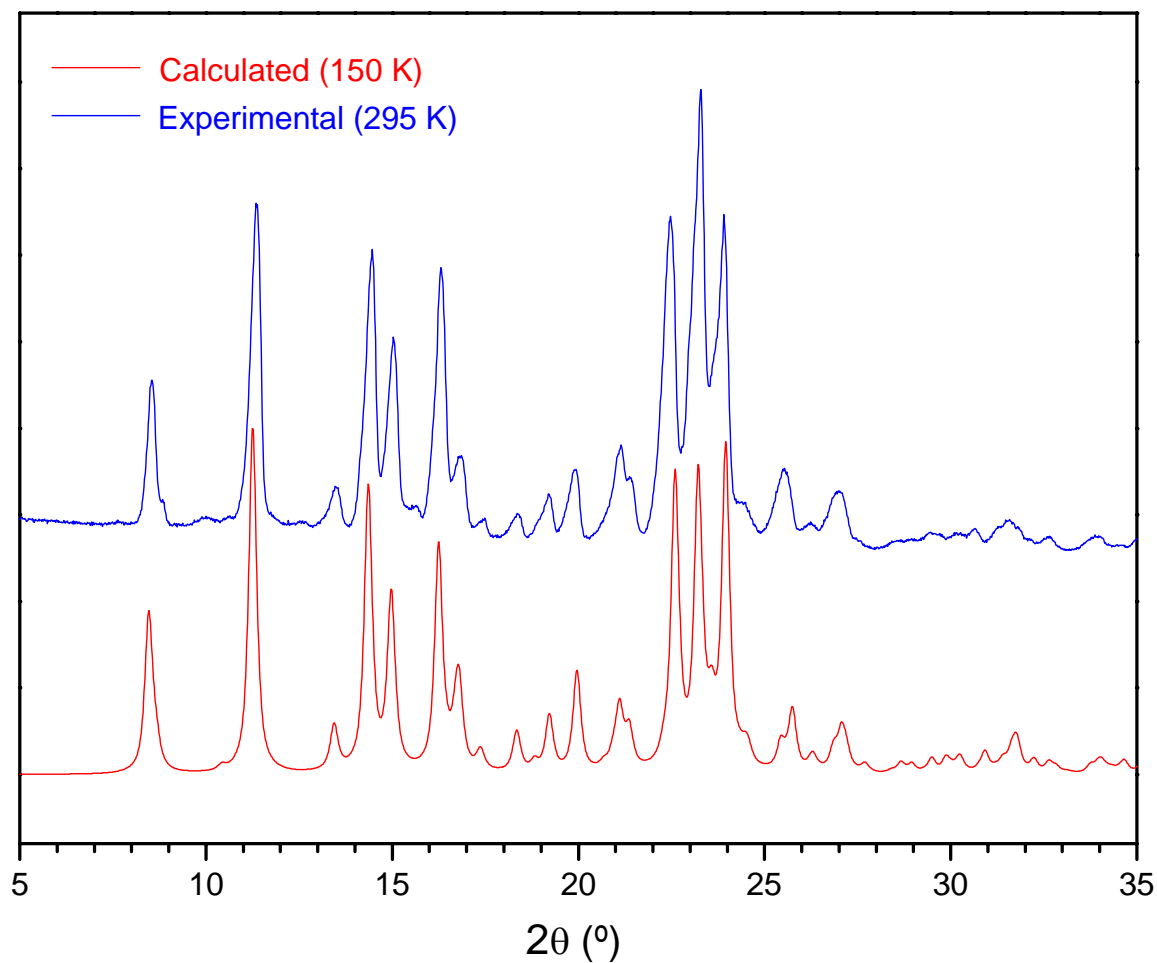
Figure S5. Comparison of experimental and calculated powder X-ray diffraction patterns of compound **3b**.

Figure S6. (a) Simulated powder X-ray diffraction pattern of crystals of compound **3b** (red curve) as determined by Pawley fitting of the experimental powder X-ray diffraction pattern (nearly superimposed blue curve). (b) Difference between experimental and calculated intensities. (c) Position of calculated reflections.

Table S1. Crystallographic Data for Compound **3b** as Determined by Pawley Fitting of Powder X-Ray Diffraction Data at 295 K.

Compound	$C_{43}H_{32}$
temperature (K)	295
crystal system	orthorhombic
space group	$Pna2_1$
a (Å)	12.4098 (29)
b (Å)	11.7731 (34)
c (Å)	21.1504 (45)
α (°)	90
β (°)	90
γ (°)	90
V (Å^3)	3090.1 (13)
Z	4

PXRD Data for Compound **3c**

Figure S7. Comparison of experimental and calculated powder X-ray diffraction patterns of compound **3c**.
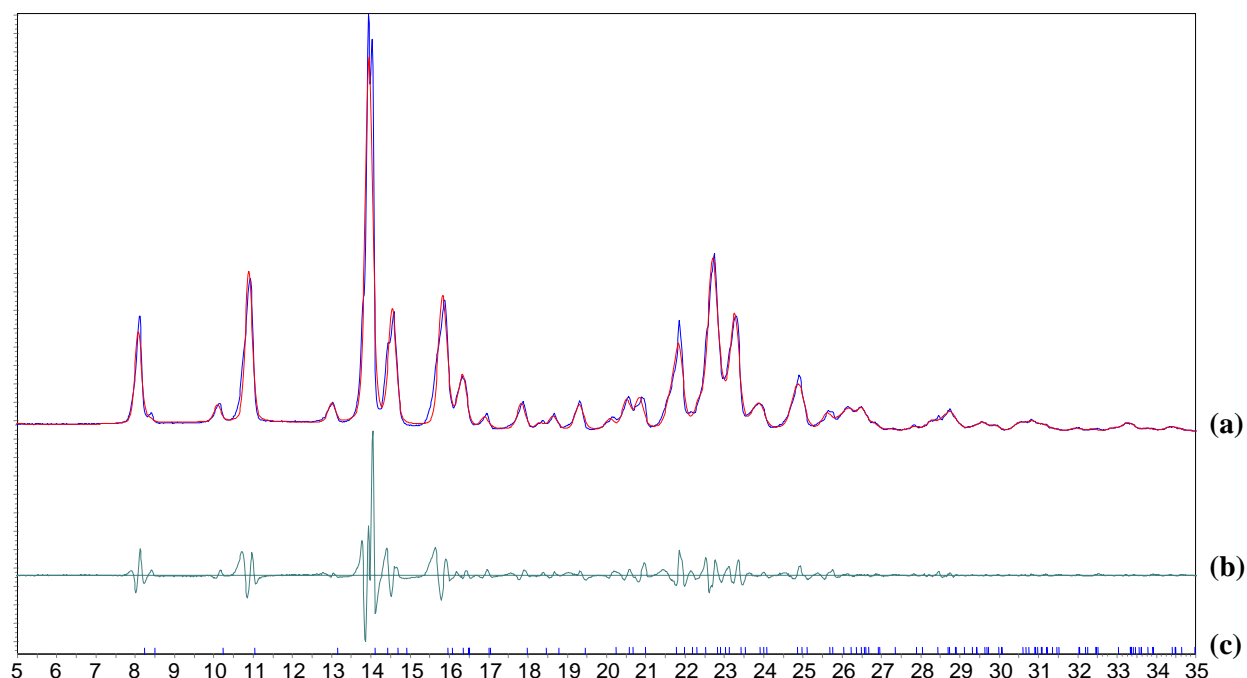
Figure S8. (a) Simulated powder X-ray diffraction pattern of crystals of compound **3c** (red curve) as determined by Pawley fitting of the experimental powder X-ray diffraction pattern (nearly superimposed blue curve). (b) Difference between experimental and calculated intensities. (c) Position of calculated reflections.

Table S2. Crystallographic Data for Compound **3c** as Determined by Pawley Fitting of Powder X-Ray Diffraction Data at 295 K.

| Compound	$C_{44}H_{34}$
temperature (K)	295
crystal system	orthorhombic
space group	$Pna2_1$
a (Å)	12.5493 (32)
b (Å)	11.8791 (45)
c (Å)	21.4742 (67)
α (°)	90
β (°)	90
γ (°)	90
V (Å^3)	3201.3 (18)
Z	4

PXRD Data for Compound **3d**
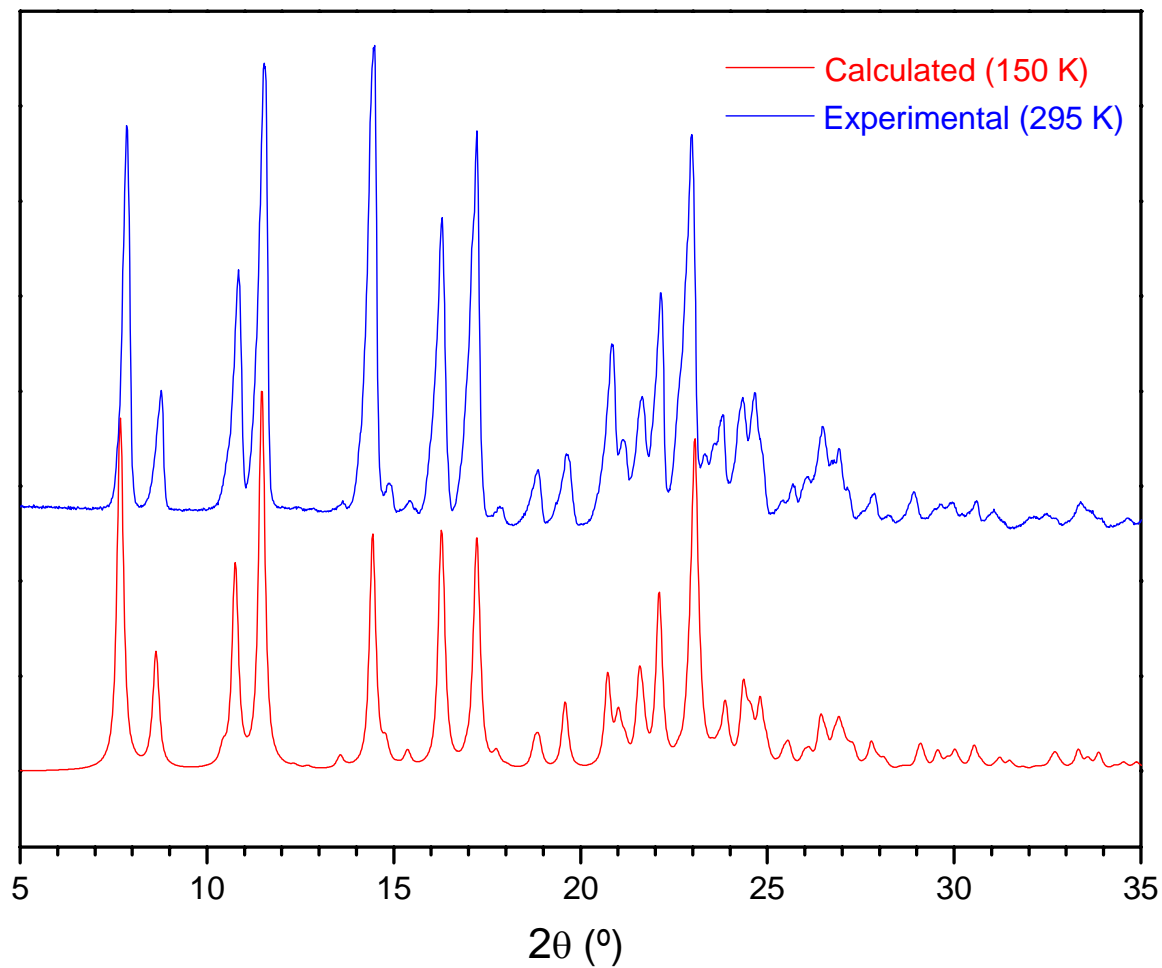
Figure S9. Comparison of experimental and calculated powder X-ray diffraction patterns of compound **3d**.
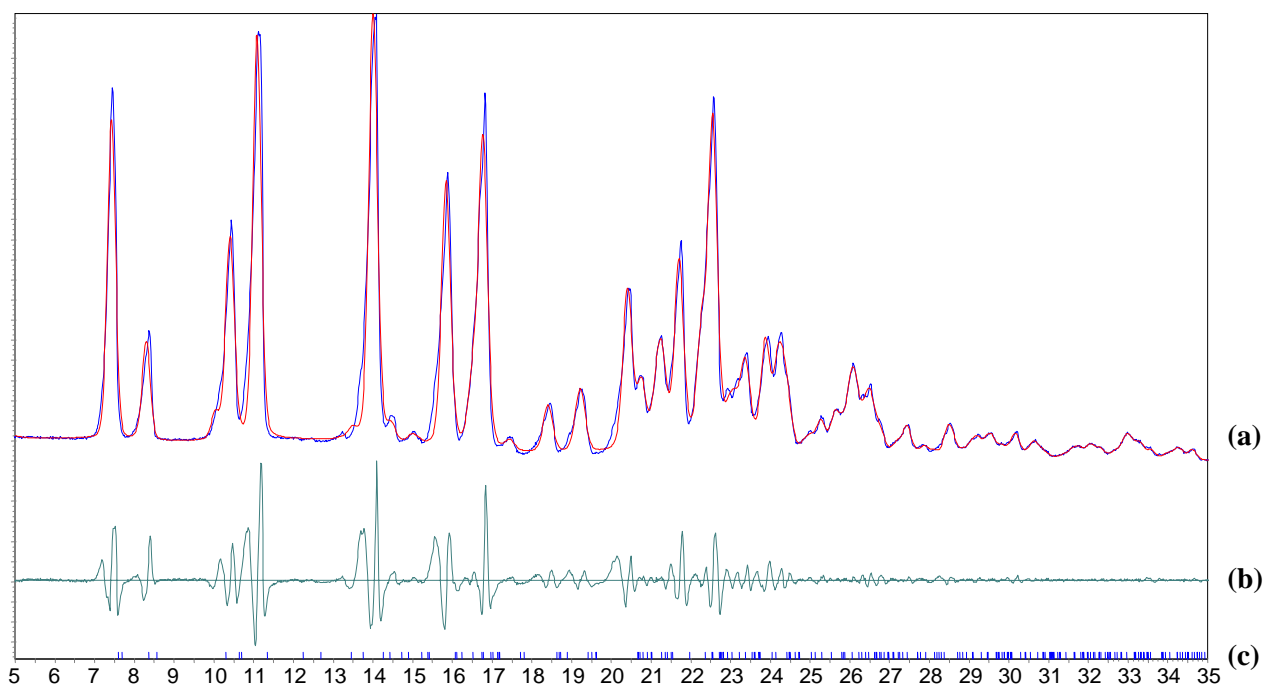
Figure S10. (a) Simulated powder X-ray diffraction pattern of crystals of compound **3d** (red curve) as determined by Pawley fitting of the experimental powder X-ray diffraction pattern (nearly superimposed blue curve). (b) Difference between experimental and calculated intensities. (c) Position of calculated reflections.

Table S3. Crystallographic Data for Compound **3d** as Determined by Pawley Fitting of Powder X-Ray Diffraction Data at 295 K.

Compound	$C_{46}H_{38}$
temperature (K)	295
crystal system	monoclinic
space group	$P2_1/n$
a (Å)	12.535 (13)
b (Å)	11.889 (13)
c (Å)	23.200 (37)
α (°)	90
β (°)	98.15 (12)
γ (°)	90
V (Å^3)	3422.6 (76)
Z	4

PXRD Data for Compound **3e**
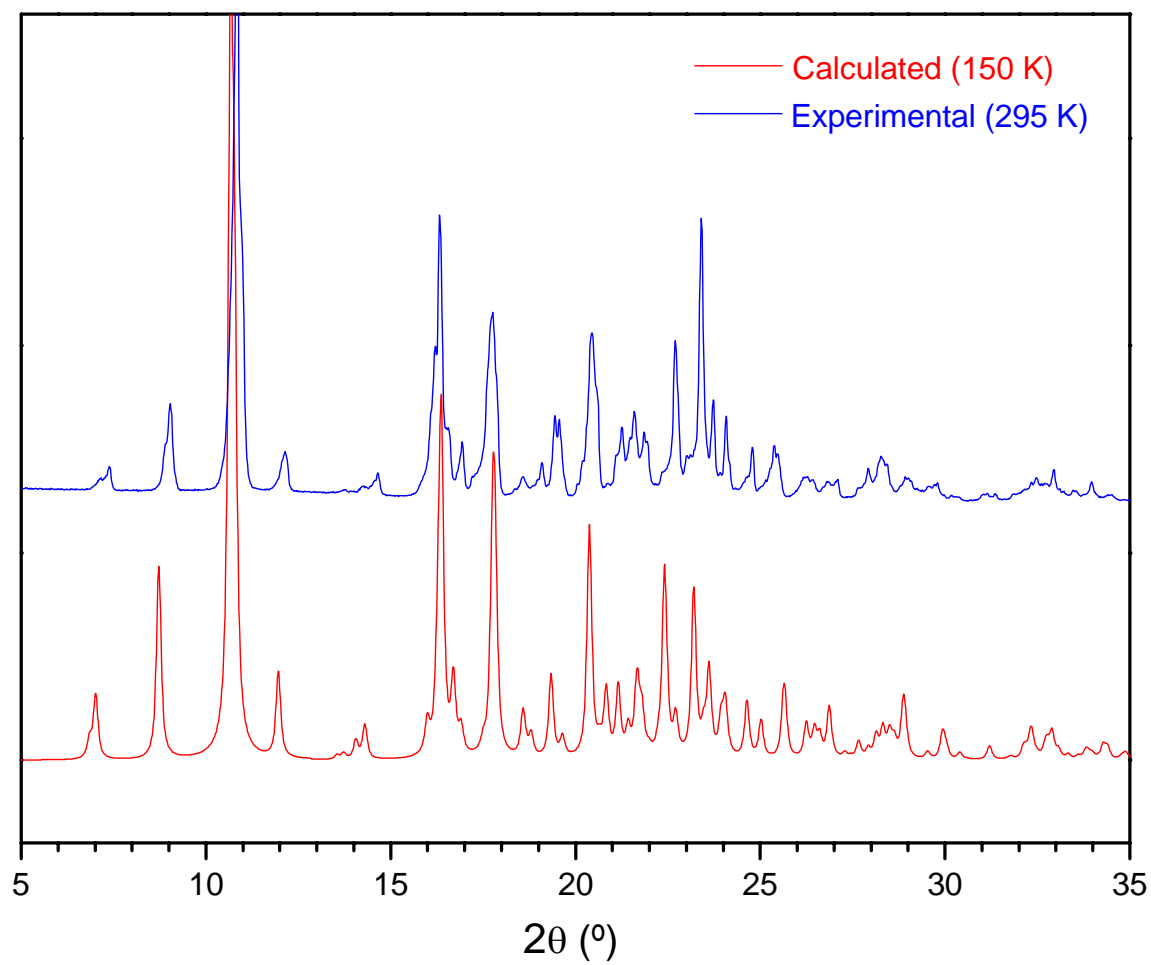
Figure S11. Comparison of experimental and calculated powder X-ray diffraction patterns of compound **3e**.
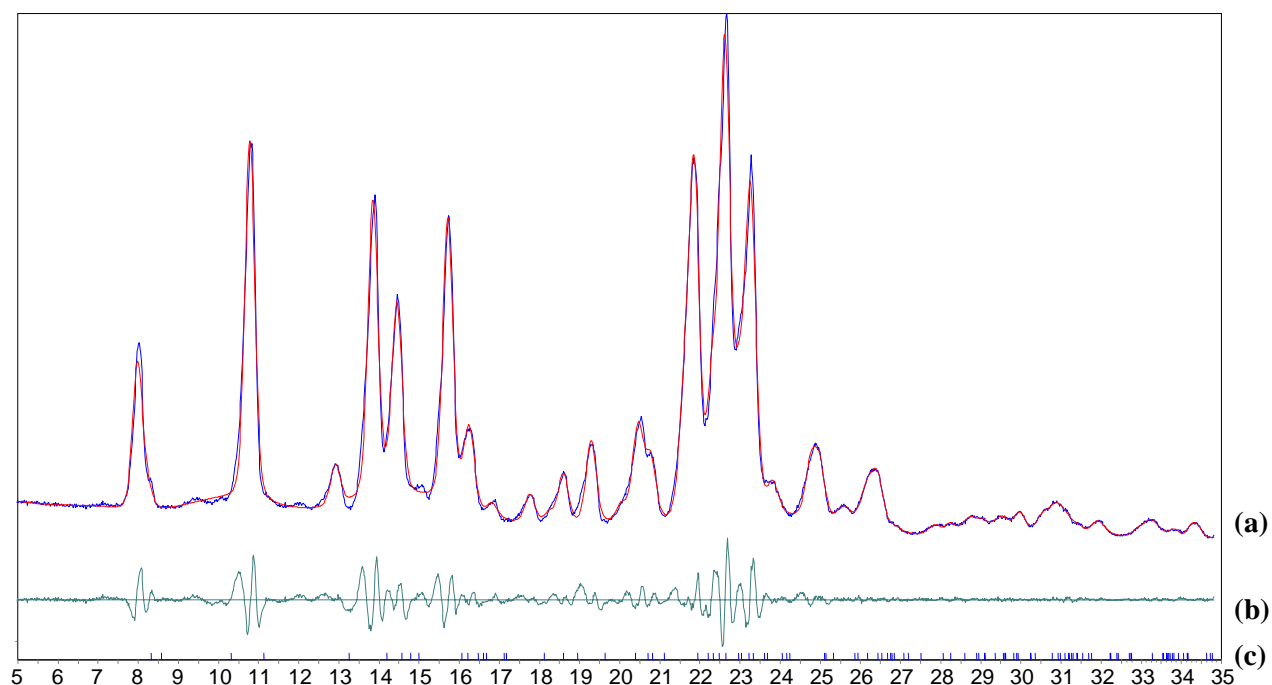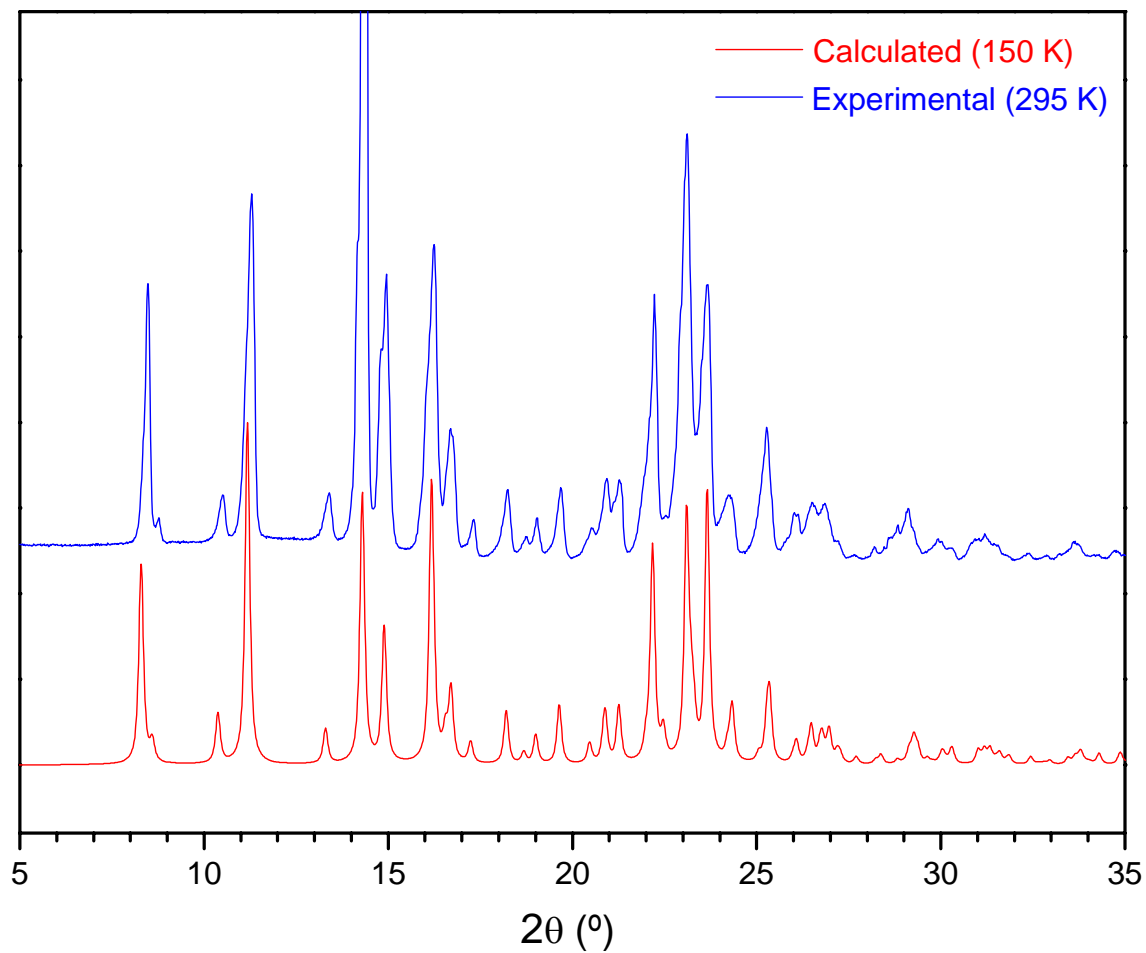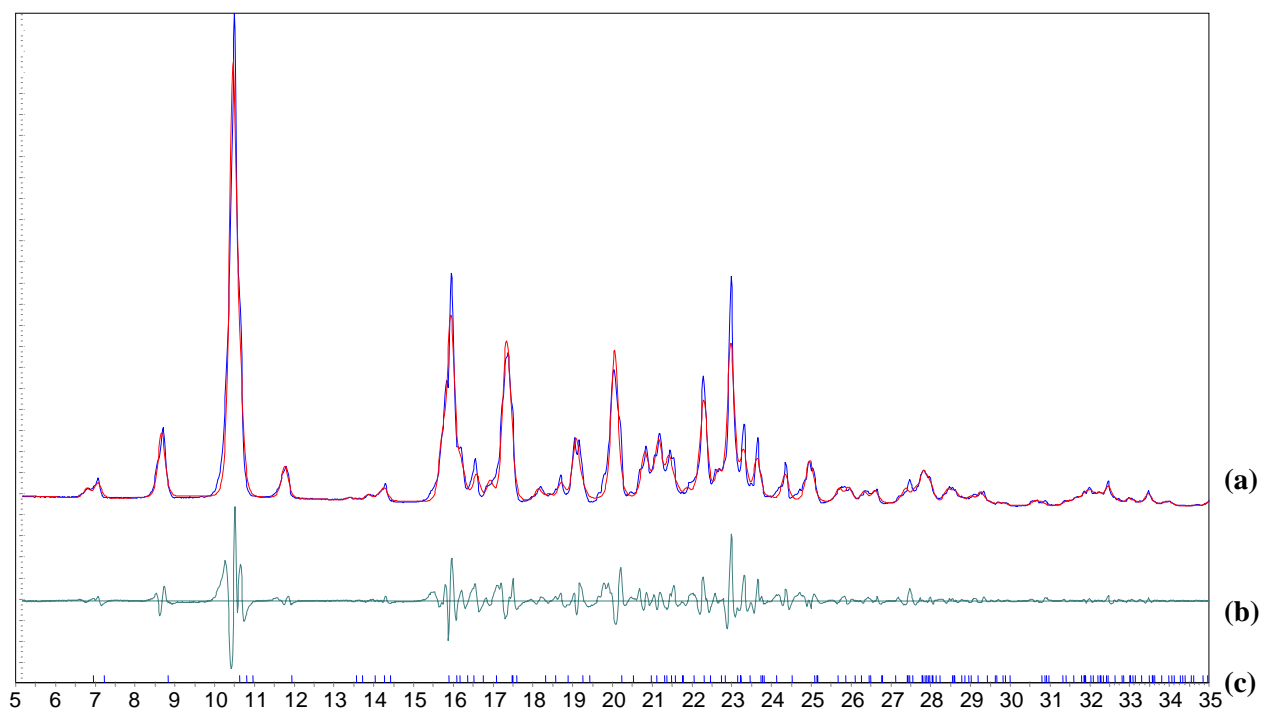
Figure S12. (a) Simulated powder X-ray diffraction pattern of crystals of compound **3e** (red curve) as determined by Pawley fitting of the experimental powder X-ray diffraction pattern (nearly superimposed blue curve). (b) Difference between experimental and calculated intensities. (c) Position of calculated reflections.

Table S4. Crystallographic Data for Compound **3e** as Determined by Pawley Fitting of Powder X-Ray Diffraction Data at 295 K.

Compound	$C_{48}H_{42}$
temperature (K)	295
crystal system	monoclinic
space group	$P2_1$
a (Å)	12.8232 (30)
b (Å)	11.0875 (45)
c (Å)	13.3414 (32)
α (°)	90
β (°)	102.489 (17)
γ (°)	90
V (Å^3)	1851.96 (98)
Z	2

3b
^{1}H NMR, CDCl$_3$, 400 MHz

7.2599
7.2561
6.993
6.9243
6.916
6.8560
6.8836
6.8202
6.8156
6.7946
6.7818

2.0282

1.5322

29.23

2.996

PPM   9.0   8.0   7.0   6.0   5.0   4.0   3.0   2.0   1.0

3b
^{13}C NMR, CDCl$_3$, 175 MHz

141.0786
140.7880
140.5218
140.4287
140.3947
140.1786
140.1785
140.0345
139.8559
139.8356
135.1535
132.1533
131.7144
131.6247
131.5000
131.5879
130.4857
130.4059
128.9459
128.7066
126.6475
126.5527
126.5313
126.4237
126.2680
125.4237
125.2656
124.0786

76.9786
77.1660
77.3414

20.8723

PPM   180   160   140   120   100   80   60   40   20

3c
^{1}H NMR, CDCl$_3$, 400 MHz

7.2601
6.8711
6.8618
6.8557
6.8497
6.8467
6.8363
6.8286
6.8257
6.8159
6.8130
6.8094
6.8067
6.8011
6.7937
6.7888
6.7937
6.7727
6.7552
6.7352
6.7335
6.6499
6.6312

2.1024

1.5528

2.060
1.058
5.058

5.947

PPM 9.0 8.0 7.0 6.0 5.0 4.0 3.0 2.0 1.0

3c
^{13}C NMR, benzene-d_6, 175 MHz

141.5766
141.3484
141.3294
141.2729
141.1272
140.8739
140.7678
140.3642
140.1044
139.3437
136.1044
132.1320
132.0642
130.8475
130.1976
128.1976
128.0600
127.9225
127.2777
127.2613
127.2226
127.1087
126.9032
126.2158
125.7954
125.7750

21.7902

PPM 180 160 140 120 100 80 60 40 20

3d

^{1}H NMR, CDCl$_3$, 400 MHz

7.2600
7.0563
6.9759
6.9426
6.9234
6.9044
6.8698
6.8658
6.8569
6.8481
6.8453
6.8447
6.8309
6.8267
6.8172
6.8089
6.7977
6.7952
6.7850

2.4928
2.4740
2.4552
2.4365

1.5204

1.0801
1.0614
1.0425

27.00
1.009

3.981

5.935

| PPM | 9.0 | 8.0 | 7.0 | 6.0 | 5.0 | 4.0 | 3.0 | 2.0 | 1.0 |

3d

^{13}C NMR, CDCl$_3$, 175 MHz

140.9872
140.8991
140.8435
140.7328
140.3952
140.3362
140.2768
140.1426
139.1426
138.2644

131.7644
131.7311
130.7388
130.7311

126.8615
126.6562
126.6504
126.3287
125.5690
125.5208
125.1955

123.3284

76.9790
77.1604
77.3419

26.1340

13.3576

| PPM | 180 | 160 | 140 | 120 | 100 | 80 | 60 | 40 | 20 |

3e
^{1}H NMR, CDCl$_3$, 400 MHz

7.2601
7.1135
7.0941
7.0749
6.8756
6.8713
6.8599
6.8520
6.8423
6.8385
6.8339
6.8209
6.7983
6.7928
6.7870
6.7849
6.7810
6.7776
6.7716
6.7681
6.7626

2.8841
2.8683
2.8513
2.8346
2.8179
2.8013
2.7838

1.5197

0.8544
0.8712

1.013
27.00

2.028

11.91

PPM   9.0   8.0   7.0   6.0   5.0   4.0   3.0   2.0   1.0

3e
^{13}C NMR, benzene-d_6, 175 MHz

146.8921
145.9565
141.8429
141.6519
141.5462
141.3033
140.4391
138.1606
137.2643
132.7715
132.4263
132.0149
128.7152
128.1976
128.0600
127.9225
127.2652
127.2240
126.9400
126.1606
125.7360
125.6942
123.4350

30.7632

25.1275

PPM   180   160   140   120   100   80   60   40   20

7.1003
7.1189
7.2075
7.2251
7.2279
7.2455
7.2589
7.2599
7.3594
7.3603
7.3613
7.3634
7.3784
7.3795
7.3804
7.3812
7.5389
7.5399
7.5427
7.5585
7.5630

2.8964
2.9153
2.9342
2.9530

1.3061
1.3251
1.3439

7

^{1}H NMR, CDCl$_3$, 400 MHz

1.984
1.956
3.000
0.974
1.956

4.028

5.992

PPM 9.0 8.0 7.0 6.0 5.0 4.0 3.0 2.0 1.0

146.6519

131.4622
128.5126
128.3859
128.1710
125.4701
124.0958
121.6365

96.9917

86.7869

77.4730
77.1555
76.8379

28.2754

14.9925

7

^{13}C NMR, CDCl$_3$, 100 MHz

PPM 180 160 140 120 100 80 60 40 20

8
¹H NMR, CDCl₃, 400 MHz

8
¹³C NMR, CDCl₃, 100 MHz

9

^{1}H NMR, CDCl$_3$, 400 MHz

7.2660
7.2640
7.2450
7.2260
7.0925
7.0735

3.4647
3.4477
3.4307
3.4137
3.3997
3.3797
3.3626

1.2498
1.2337
1.2327

1.326
1.995

2.000

12.27

PPM 9.0 8.0 7.0 6.0 5.0 4.0 3.0 2.0 1.0

9

^{13}C NMR, CDCl$_3$, 100 MHz

151.2482

128.4657
123.9412

109.3452

76.8401
77.1575
77.4751

39.5466

23.5266

PPM 180 160 140 120 100 80 60 40 20